

Dark Initial State Radiation and the Kinetic Mixing Portal

Thomas G. Rizzo [†]

SLAC National Accelerator Laboratory
2575 Sand Hill Rd., Menlo Park, CA, 94025 USA

Abstract

Data from Planck measurements of the cosmic microwave background (CMB) place important constraints on models with light dark matter (DM) and light mediators especially when both lie in the mass range below ~ 1 GeV. In models involving kinetic mixing where the dark photon acts as the mediator, these constraints are easily satisfied and the appropriate DM relic density achievable if the DM is, *e.g.*, a complex scalar, where p -wave annihilation occurs, or is the lighter component of a split pseudo-Dirac state where co-annihilation dominates. In both of these cases, although higher order in the dark gauge coupling, g_D , the corresponding annihilation processes including dark photon initial state radiation (ISR) will be dominantly s -wave with essentially temperature independent cross sections. The rates for these dark ISR associated processes, though not yielding cross sections large enough to contribute to the relic density, can still run into possible conflicts with the bounds arising from the CMB. In this paper we perform a preliminary study of the present and potential future constraints that the CMB imposes on the parameter spaces for both of these scenarios due to the existence of this dark ISR. Further analyses of the effects of dark ISR in DM annihilation is clearly warranted.

[†]rizzo@slac.stanford.edu

1 Introduction

The nature of dark Matter (DM) and its possible interactions with the particles of the Standard Model (SM) other than via gravity remains a great mystery. While Weakly Interacting Massive Particles (WIMPs) [1, 2] and axions [3–5] remain as quite viable contenders for the role of DM, increasingly sensitive experiments have failed to yield any convincing signals [6–8] for these long anticipated states. The continued shrinking of the allowed parameter spaces for these scenarios has stimulated a rapid growth of new DM models covering exceedingly wide ranges in both possible masses and couplings [9–12]. As current experiments seemingly disfavor the interaction of DM with us via SM strength couplings, other new interactions must likely exist to explain, *e.g.*, how DM reaches its observed relic abundance [13, 14]. One way to classify such new interactions is via a set of ‘portals’ linking the SM with fields in the dark sector. Only a few renormalizable, dimension-4 portals exists; of these, the vector boson/kinetic mixing (KM) portal has received a wide amount of attention in the literature [15, 16] and will be the subject of our discussion below. In the simplest version of such a scenario, the DM fields are SM singlets but are instead charged under a new $U(1)_D$ gauge interaction, with corresponding gauge coupling g_D , mediated by a dark photon (DP) [17] whose mass can be generated by the dark analog of the SM Higgs mechanism. This DP then kinetically mixes with the SM $U(1)_Y$ hypercharge gauge boson at, *e.g.*, the 1-loop level via a set of ‘portal matter’ fields which are charged under both gauge groups [18–20]. After the gauge fields are canonically normalized and the usual SM and dark spontaneous symmetry breakings occur, the DP picks up a small coupling to the SM fields. For a DP in the mass range below a few GeV, this coupling is quite well approximated simply by $\simeq \epsilon e Q_{em}$, where ϵ is a small dimensionless parameter, $\sim 10^{-(3-4)}$ in the present discussion, that describes the magnitude of this loop-suppressed KM.

The KM scenario is of special interest when the DM and DP are both relatively light $\lesssim 1$ GeV as in such a case the DM can be a thermal relic in a manner similar to what occurs in the WIMP scenario¹. For such a range of masses, pair annihilation of DM to achieve the proper relic density via the exchange of a virtual DP usually results in pairs of electrons, muons, or light charged hadrons. For DM at the $\sim 10 - 1000$ MeV mass scale², constraints from Planck [22] on the CMB tell us that at $z \sim 10^3$ the DM annihilation cross section into light charged states, *e.g.*, e^+e^- , must be relatively suppressed [23, 24] to avoid injecting additional electromagnetic energy into the plasma. This constraint lies roughly [25] at the level of $\sim 5 \times 10^{-29} (m_{DM}/100 \text{ MeV}) \text{ cm}^3\text{s}^{-1}$, and is seen to depend approximately linearly on the DM mass so that it becomes relatively ineffective above masses $\gtrsim 10 - 30$ GeV. This constraint for DM in this $\sim 10 - 1000$ MeV mass range, however, lies several orders of magnitude below the cross section required to reach the observed relic density during freeze out, *e.g.*, $\langle \sigma v_{rel} \rangle_{FO} \simeq 4.4(7.5) \times 10^{-26} \text{ cm}^3\text{s}^{-1}$ for an *s*-wave annihilating, self-conjugate fermion (or a *p*-wave annihilating complex scalar) DM [13, 14]. This requirement puts a strong constraint on the nature of the DM interacting with the SM via the DP as well as on their relative masses. For example, if $m_{DM} > m_{DP}$, then DM can annihilate into a pair of DPs which will likely be the dominant mechanism to achieve the observed relic density. As an *s*-wave process, the cross section for this reaction during freeze out and during the time of the CMB would naturally be quite similar and so this reaction, as well as those for other *s*-wave annihilation processes, would necessarily be forbidden for light DM by the above mentioned constraints. Clearly a set of mechanisms that reduce the DM annihilation cross section as the temperature, T , decreases are required. One obvious way to avoid this constraint is to require that $m_{DM} < m_{DP}$ and also that the *s*-channel DP-mediated annihilation process be *p*-wave so that it is velocity-squared suppressed at times much later than freeze out; this is quite helpful since $v_{rel}^2 \sim T$. This possibility restricts the DM to be a Majorana fermion (which can only have axial-vector couplings to the DP and is not realized within the present context) or a complex scalar, ϕ . Note that since Dirac fermion DM annihilation via an *s*-channel, spin-1 exchange with only vector couplings is dominantly *s*-wave, this possibility is forbidden within the above range of masses. A second scenario is that the DM is pseudo-Dirac, forming two mass eigenstates, $\chi_{1,2}$, that are split in mass and which co-annihilate to the SM via the DP. For a fixed mass splitting, as the temperature drops this co-annihilation process becomes highly Boltzmann suppressed thus avoiding the CMB constraints. The parameter spaces of these two classes of models for light DM/DP in the mass range of interest to

¹The DP and DM masses are naturally similar in several scenarios, *e.g.*, models with extra dimensions where the scale of their masses is set by the (inverse) size of the compactification scale, R .

²The rough lower bound on the DM mass of ~ 10 MeV is taken from Ref. [21]

us here have been widely studied [10, 11] and it is known that the observed relic density is achievable in both these setups while still satisfying all other existing experimental constraints.

For SM singlet DM, the lifting of velocity (and/or helicity) suppression of DM annihilation in many models via the final state radiation (FSR) of SM gauge bosons off of other SM fields in the final state is well-known [26–28]. In our mass range of interest, the only possible on-shell FSR would be via photons being radiated off of, *e.g.*, an e^+e^- , $\mu^+\mu^-$ or light charged hadron final state. Less well studied, but of similar, and in some cases more, importance is the initial state radiation (ISR) of the dark mediator field, here the DP, off of the annihilating DM [29]. Note that since the DM can only be a SM singlet in the present scenario, such ISR *must* necessarily be dark at tree-level. Given the discussion above, this process can obviously be of most relevance to us when $m_{DM} < m_{DP} < 2m_{DM}$ which is a relatively narrow mass window but is of important experimental interest since within it any DPs produced on-shell can decay only to SM final states. There are many existing and proposed searches for such classes of events [30–37].

We note, and as will be examined further below, that dark ISR can, in principle, lead to some affects which are not possible via FSR: (i) In the case of complex scalar DM, FSR cannot lift the p -wave suppression since this is the result of the (non-relativistic) coupling of the two spin-0, on-shell initial states with the spin-1, off-shell DP. This is easy to see as in the non-relativistic limit, the usual scalar coupling, $(p_1 - p_2)_\mu$ has, to $O(v_{rel}^2)$, only non-zero 3-spatial components, $\simeq m_{DM}v_{rel}$, so that this automatically leads to a p -wave process. Dark ISR changes this situation in that now one of the DM particles in the initial state annihilating via the virtual DP, itself goes off-shell. We now make a rather simple observation: although this process is $\sim g_D^2/4\pi^3 = \alpha_D/\pi$ suppressed it is still dominantly an s -wave annihilation mechanism, though it is too small to make any significant contribution to the DM relic density. However, it can yield a rate which is sufficiently large so as to be in potential conflict with the CMB constraints above and thus lead to restrictions on the model parameter space; we will examine this possibility below. (ii) Similarly, in the case of pseudo-Dirac DM, the two DM mass eigenstates couple in an off-diagonal manner to the DP while the ‘diagonal’ couplings, which would be unsuppressed s -wave annihilations, are absent at lowest order in g_D . It is well known that obtaining the observed relic density via the co-annihilation process requires that the relative mass splitting of these two eigenstates be relatively small, *i.e.*, $\delta = \Delta m/m_{DM} \ll 1$. If not, this process becomes highly Boltzmann suppressed by a factor of order $\sim e^{-\delta x_f}$ with $x_f = m_{DM}/T_{FO} \simeq 20 - 30$. As we will see below, dark ISR may partially negate this (very) large Boltzmann suppression even in cases where this mass splitting is no longer so small, *i.e.*, $\delta \lesssim 0.1 - 1$, but at the cost of this additional power of $\sim \alpha_D/\pi$. The resulting rate is, however, too small to make a significant contribution to the relic density. But in this case too, an s -wave process is the net result so that the question again arises as to whether or not the bounds from the CMB remain satisfied once ISR of a DP occurs. We will address this issue within this model context in the subsequent analysis as well. Clearly the implications of ISR dark radiation for the allowed parameter space of a given DM model warrants some further examination and that is goal of the preliminary analysis below.

The outline of this paper is as follows: in Section 2, we will discuss the general overarching model structure that we will consider and then immediately turn our attention to the specific case of complex scalar DM. In particular, we will explore the extent to which dark ISR can lead to conflicts with the constraints arising from the CMB and the corresponding restrictions this imposes on the complex DM model parameter space. Similarly, in Section 3, we will explore the impact of dark ISR in the case of pseudo-Dirac DM wherein co-annihilation is the dominant process leading to the observed relic density. We again will examine the possible conflict with the CMB constraints that can arise and which lead to restrictions on the model parameter space even in cases where the mass splitting between the two eigenstates is significant and contrast this with the previously examined case of complex scalar DM. A discussion and our conclusions can be found in Section 4.

2 General Model Features and the Complex Scalar DM Scenario

We first briefly summarize the common features of the basic framework that we consider below, restate our essential assumptions and then establish subsequent notation before continuing with our analysis.

2.1 Basic Setup

The interactions in the (mostly) dark gauge/Higgs sector of our model in the original weak eigenstate basis are described by the general Lagrangian

$$L = -\frac{1}{4}\hat{V}_{\mu\nu}\hat{V}^{\mu\nu} - \frac{1}{4}\hat{B}_{\mu\nu}\hat{B}^{\mu\nu} + \frac{\epsilon}{2c_w}\hat{V}_{\mu\nu}\hat{B}^{\mu\nu} + (D_\mu S)^\dagger(D^\mu S) - U(S^\dagger S) - \lambda_{HS}H^\dagger HS^\dagger S + L_{SM}, \quad (1)$$

where \hat{V}, \hat{B} are the kinetically mixed $U(1)_D$ DP and the SM weak $U(1)_Y$ hypercharge gauge fields, respectively, with the strength of this KM being described by the dimensionless parameter ϵ ; here $c_w = \cos\theta_w$ with θ_w being the usual SM weak mixing angle. Since we will assume that the KM parameter is very small in what follows, $\epsilon \simeq 10^{-(3-4)}$, except where necessary we can work to leading order in ϵ . In this limit the KM is removed by the simplified field redefinitions $\hat{B} \rightarrow B + \frac{\epsilon}{c_w}V$, $\hat{V} \rightarrow V$. H, S denote the SM and dark Higgs fields, respectively, while L_{SM} describes the rest of the interactions of the SM. The vacuum expectation value of S , $v_s/\sqrt{2}$, resulting from minimizing the potential U , generates the mass of the DP, $m_{DP} = m_V = g_D Q_D(S)v_s$, via the dark covariant derivative $D_\mu = \partial_\mu + ig_D Q_D(S)\hat{V}_\mu$. Here, g_D is the $U(1)_D$ gauge coupling and $Q_D(S)$ is the relevant dark charge of S . Due to the vevs of both H and S , $\lambda_{HS} \neq 0$ generates a mass mixing between the SM and dark Higgs fields which we will necessarily assume to be very small to avoid the strong bounds arising from invisible Higgs decays [38] and so will be considered to be phenomenologically irrelevant in the subsequent discussion. It will also be assumed that $m_S > (1-2)m_V$, similar to what happens in the SM, so that S is guaranteed to be unstable and can decay sufficiently rapidly as, *e.g.*, $S \rightarrow 2V$ (or $\rightarrow VV^*$) although the specific details of this will not be required for the discussion below.

2.2 Complex DM

While the form of L above is quite general, the addition of the DM itself will introduce some new terms to this set of interactions. In this subsection, we consider the case where the DM is a complex scalar, ϕ ; the form of the general additional pieces of the Lagrangian in this case are given by

$$L_{DM} = (D_\mu \phi)^\dagger(D^\mu \phi) - U_\phi(\phi^\dagger \phi) - (\lambda_{H\phi}H^\dagger H + \lambda_{\phi S}S^\dagger S)\phi^\dagger \phi, \quad (2)$$

where D_μ is the relevant covariant derivative for ϕ , whose dark charge will be taken to be unity in what follows without loss of generality. The potential U_ϕ describes the (taken to be weak) DM self-interactions which we assume do not generate a vev for ϕ so that it can remain stable. The quartic couplings of ϕ with both S and H , described by the coefficients $\lambda_{\phi(S,H)}$, respectively, will also be assumed to be quite small and to play no essential role in what follows.

Under this set of assumptions, the DM-DP gauge interaction completely dominates and leads to a slightly modified version of the well-known expression [39] for the annihilation cross section of scalar DM pairs into SM fields in our mass range of interest; summing over electron, muon and light charged hadronic final states, this is given by

$$\sigma_{DM}v_{rel} = \frac{g_D^2 \epsilon^2 e^2}{6\pi} \frac{s\beta_\phi^2}{(s - m_V^2)^2 + (\Gamma_V m_V)^2} \left[1 + \frac{\beta_\mu(3 - \beta_\mu^2)}{2} \theta(s - 4m_\mu^2) + R \theta(s - 4m_\pi^2) \right], \quad (3)$$

where s is the usual center of mass energy, $\beta_{\phi,\mu}^2 = 1 - 4m_{\phi,\mu}^2/s$ are the squares of the DM (muon) velocities, Γ_V is the total decay width of the DP, and R is the familiar cross section ratio $R = \sigma(e^+e^- \rightarrow \text{hadrons})/\sigma(e^+e^- \rightarrow \mu^+\mu^-)$ via virtual photon exchange for massless muons. Of course, this hadronic contribution only turns on above the two-pion threshold; note that the electron mass has been neglected in the expression for $\sigma_{DM}v_{rel}$. Here we observe the explicit β_ϕ^2 -dependence of the DM annihilation cross section as expected from the discussion above. Γ_V depends sensitively on the value of $r = m_\phi/m_V$ since for $r < 1/2$, the DP can decay dominantly into DM pairs with a reasonable large partial width, $\Gamma_V/m_V = g_D^2 \beta^3/48\pi$ ³, where $\beta^2 = 1 - 4r^2$. However, for larger values of r , in the region of interest to

³Here it is assumed that g_D is a typical-sized gauge coupling.

us below, only the DP decays to SM states are allowed and these modes all have partial widths that are ϵ^2 suppressed, *e.g.*, $\Gamma(V \rightarrow e^+e^-)/m_V = (\epsilon e)^2/12\pi$, when the electron mass has again been neglected.

To obtain the thermally averaged cross section leading to the DM relic density we integrate the above expression weighted by the Bose-Einstein distributions of the incoming complex DM states. Though this is p -wave suppressed, the thermal average of the above cross section can yield the observed relic density for the $1/2 < r < 1$ range of interest as is shown in Fig. 1. Special care must be taken with the resonance enhancement region [40, 41] which we take some minor advantage of in the calculation. For example, if one takes $g_D\epsilon \simeq 3 \times 10^{-4}$ and $m_V \simeq 100$ MeV, the required cross section is obtained near $r \simeq 0.75$, essentially at the center of our mass range of interest. Similar other combinations of parameter choices within the mass range $1/2 < r < 1$ can work equally well but we will employ this value, $r = 0.75$, as a rough benchmark below as it is relatively far off-resonance. Clearly, we observe that solutions also exist when $r < 1/2$ but they lie outside the specific mass region of interest to us here. Of course, this parameter space will be further constrained by other future experiments, *e.g.*, via dark photon production at accelerators or via DM direct detection experiments employing ϕ scattering off of electrons and/or nucleons.

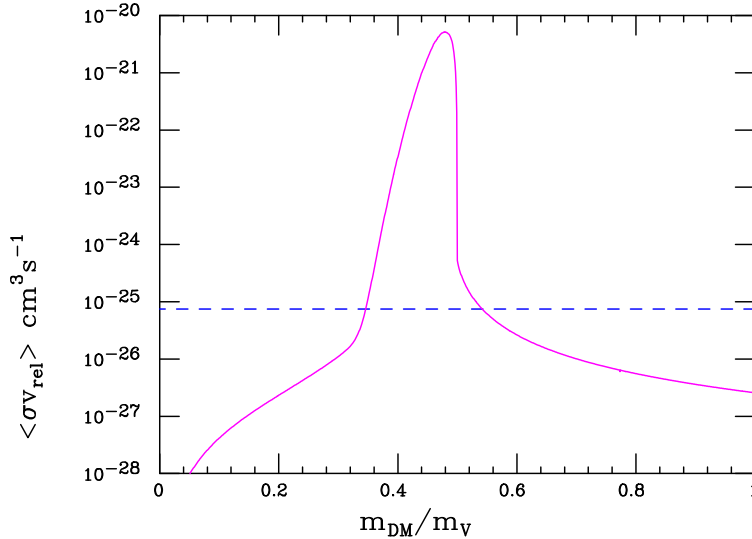


Figure 1: The thermally averaged complex scalar DM annihilation cross section assuming $m_V = 100$ MeV, $g_D\epsilon = 10^{-4}$ with $x_f = 20$. The expression in the square bracket in the text has been set to unity here. The corresponding results for other values of these input parameters can be obtained via simple rescaling using the equation in the text. The dashed line shows the approximate required annihilation cross section needed to obtain the observed relic density.

We turn now to our first example of the influence of dark ISR. Consider the specific process $\phi^\dagger\phi \rightarrow VV^*, V^* \rightarrow e^+e^-$, which occurs via both t - and u -channel DM exchanges as well as via the usual 4-point coupling. We will consider this reaction in the non-relativistic limit for the DM in the mass range of interest $1/2 < r < 1$, which is necessarily a non-resonant process; we will continue to take $m_e = 0$ for simplicity in what follows as we will always assume that $m_{\text{DM}} \gg m_e$. We note that if $\lambda_{\phi S}$, discussed above, were significant, something that we have assumed *not* to be the case here, then an additional s -channel diagram would be possible via virtual S^* exchange followed by $S^* \rightarrow VV^*$. We find, however, that even when $\lambda_{\phi S}$ is significant, this contribution would be relatively numerically suppressed (by up to one or two orders of magnitude) due to a combination of overall constant factors combined with a relative ratio of $(m_V/m_S)^4 \ll 1$ in comparison to that coming from DP exchange. In any case, we will ignore this possible contribution here.

Recall that these t -, u -channel DM exchanges added to the 4-point interaction result in an s -wave

process and so it is subject to the above mentioned constraints from the CMB. We can write the numerical result for the annihilation cross section for this reaction as

$$\sigma_{DM}v_{rel} = 1.98 \times 10^{-2} \sigma_0 \left(\frac{g_D}{e}\right)^2 \left(\frac{g_D \epsilon}{10^{-4}}\right)^2 \left(\frac{100\text{MeV}}{m_V}\right)^2 I, \quad (4)$$

where $\sigma_0 = 10^{-26} \text{ cm}^3\text{s}^{-1}$ sets the scale to that which is roughly required for the annihilation cross section to result in the observed DM relic density and I is the phase space integral

$$I = 2v^2 \int_0^{(1-v)^2} dx_{12} \int_{min}^{max} dx_{23} \frac{2(1-x_{23})(x_{12}+x_{23}-v^2)-x_{12}(1+v^2+x_{12})}{(1-x_{12}-v^2)^2[(x_{12}-v^2)^2+(Gv^2)^2]}, \quad (5)$$

where $v = 1/2r = m_V/2m_\phi$, $G = \Gamma_V/m_V$, $x_{12} = m_{ee}^2/4m_\phi^2$, with m_{ee} being the e^+e^- invariant mass in the final state, $x_{23} = 1 - E_{e-}/m_\phi$ with E_{e-} being the corresponding electron energy, and the range of the x_{23} integration is given by $(max, min) = \frac{1}{2}(1 - x_{12} + v^2) \pm \frac{1}{2}[(1 - x_{12} - v^2) - 4x_{12}v^2]^{1/2}$. In terms of the parameter v , we note that the $\phi^\dagger\phi \rightarrow V^* \rightarrow e^+e^-$ resonance region lies in the vicinity of $v \simeq 1$ while the on-shell $\phi^\dagger\phi \rightarrow 2V$ process occurs when $v \sim 1/2$ so we must lie away from both regions. Since the reaction with ISR is an s -wave process (and keeping well away from the resonance region), the thermal average cross section is essentially the same as the non-relativistic cross section itself, *i.e.*, $\langle \sigma_{DM}v_{rel} \rangle \simeq \sigma_{DM}v_{rel}$, so that numerical results can be obtained in a rather straightforward manner employing the familiar velocity expansion. This will be a very good approximation at the time of the CMB in which we are interested as higher order terms in $v^2 \sim T$ will necessarily be quite suppressed.

The top panel of Fig. 2 shows the result of this calculation obtained by taking the same set of input parameters as above, *i.e.*, $m_V = 100 \text{ MeV}$, $g_D \epsilon = 3 \times 10^{-4}$, $r = m_\phi/m_V = 0.75$ (implying that $m_\phi = 75 \text{ MeV}$ and $v \simeq 0.667$) and assuming that $g_D = g_{wk}[e]$, where g_{wk} is the SM $SU(2)[\text{QED}]$ gauge coupling, for purposes of demonstration; we then find that $\sigma_{DM}v_{rel} \simeq 2.6(0.59) \times 10^{-29} \text{ cm}^3\text{s}^{-1}$. The first of these values, while still allowed, lies relatively close to the current rough CMB bound for this DM mass as given in Ref. [25], *i.e.*, $\sim 3.5 \times 10^{-29} \text{ cm}^3\text{s}^{-1}$ while the second still lies well within a rather safe region. Thus, at present, while part of this model's parameter space will certainly be excluded by dark ISR, the existing CMB bounds are relatively weak and still remain seemingly easy to evade while simultaneously allowing for the observed relic density. As seen in the Figure, possibly significant improvement in these CMB bounds from future measurements by up to an order of magnitude [25] will increase any tension with the parameter space required to obtain the observed DM relic density, excluding the benchmark with the choice $g_D = g_{wk}$.

In order to get a more general feeling for the constraints that the existence of the dark ISR process can impose on the parameter space of this model, it is convenient to consider the dimensionless parameter η as defined by following combination of factors:

$$\eta = \alpha_D \frac{\epsilon}{10^{-4}} \left[\frac{100\text{MeV}}{m_V} \right]^{3/2}, \quad (6)$$

where $\alpha_D = g_D^2/4\pi$ as usual⁴. It is important to note the particular fundamental parameter dependence of η as defined here. Given the discussion of the DM annihilation cross section above, we might roughly expect that η generally lies in the range $\sim 0.1 - 1$. Employing the approximate form of the CMB bound discussed above and the results in the top panel of Fig. 2 we can obtain the constraints on η as shown in the lower panel of the same Figure together with the predictions for our benchmark point with either $g_D = g_{wk}$ or $g_D = e$. While the latter is quite safely inside the allowed region, the former lies close to, but still below, the boundary in the presently allowed region as we found above. Here we see that future CMB measurements will be easily able to exclude this particular parameter choice. These preliminary results show the potential impact of considering the important effects of dark ISR as part of the complete DM annihilation process in this mass range especially in determining the allowed parameter space for any given model.

⁴Note that η is somewhat similar in spirit to the parameter y used to describe the parameter space for both DP production as well as the scattering cross section in DM direct detection experiments [10, 11].

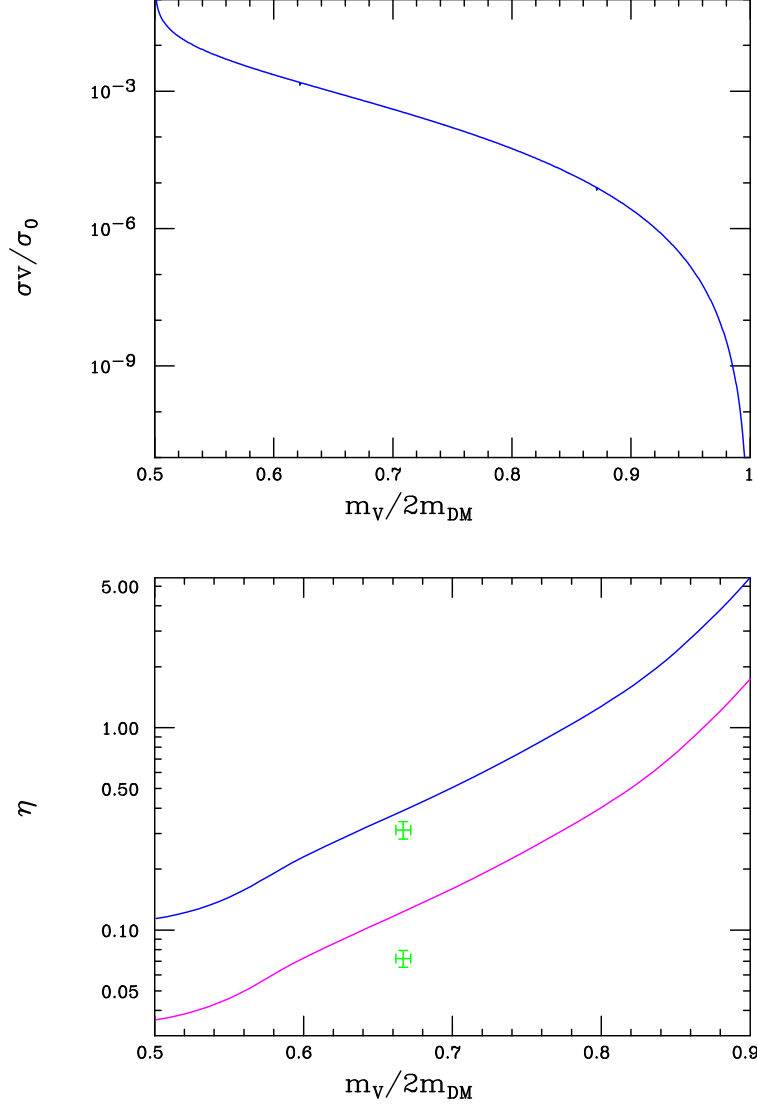


Figure 2: (Top) The annihilation cross section for the process $\phi^\dagger\phi \rightarrow VV^*, V^* \rightarrow e^+e^-$ in the non-relativistic limit assuming $m_V = 100$ MeV, $g_D\epsilon = 10^{-4}$ and $g_D/e = 1$ for purposes of demonstration as a function of the ratio $v = m_V/2m_\phi$. Here $\sigma_0 = 10^{-26} \text{ cm}^3\text{s}^{-1}$ sets the overall cross section scale. The cross section for other parameter choices can be obtained by simple rescaling, employing the formula given in the text. (Bottom) Present (potential future) upper bound on the dimensionless parameter η described in the text as a function of $v = m_V/2m_\phi$ corresponding to the upper (lower) curve, respectively. The benchmarks for η shown here correspond to the two parameter choices discussed in the text where $r = 0.75$, $m_1 = 100$ MeV, $g_D\epsilon = 3 \times 10^{-4}$ and with $g_D = g_{wk}(e)$ corresponding to the upper (lower) point.

3 Pseudo-Dirac Scenario

We now turn to the case of a pseudo-Dirac DM particle; here the complex scalar part of L_{DM} above is replaced by

$$L_{DM} = i\bar{\chi}\gamma^\mu D_\mu\chi - m_D\bar{\chi}\chi - (y_s\bar{\chi}\chi^c S + h.c.), \quad (7)$$

where, in addition to the $U(1)_D$ -invariant Dirac mass, m_D , we assume that an additional Majorana mass term, m_M , is generated by χ 's coupling to S after it obtains the dark Higgs vev, v_s . For this to happen, of course, we need to require that $2Q_D(\chi) + Q_D(S) = 0$ which is easily arranged. In such a case, the Dirac field χ splits into two distinct mass eigenstates: $\chi = (\chi_1 + i\chi_2)/\sqrt{2}i$ and $\chi^c = i(\chi_1 - i\chi_2)/\sqrt{2}$, with $m_{1,2} = m_D \mp m_M$ where $m_M = y_s v_s/\sqrt{2}$ and y_s being a (assumed real) Yukawa coupling⁵. The fractional mass splitting between these two states is then simply $\delta = (m_2 - m_1)/m_1 = 2m_M/m_1$ which may, in principle, be $O(1)$ or even larger. For values of $\delta \gtrsim 0.01 - 0.05$ or so, it is unlikely that any signal would be obtained in this scenario from direct detection experiments [42] at tree level since the DM trapped in the galaxy would have insufficient velocity to excite the higher mass state. Here χ_1 is identified with the stable DM whereas χ_2 can now decay to χ_1 plus a (possibly on-shell) DP due to an off-diagonal interaction. For small δ , where V is clearly off-shell, this lifetime can be fairly long since the decay width roughly scales as $\sim (g_D e\epsilon)^2 \delta^5$ [43, 44]. In the mass eigenstate basis, this leading off-diagonal interaction of $\chi_{1,2}$ with the DP, V , is given by

$$L_{int} = ig_D (\bar{\chi}_1 \gamma_\mu \chi_2 - \bar{\chi}_2 \gamma_\mu \chi_1) V^\mu, \quad (8)$$

from which we see immediately why co-annihilation via virtual V -exchange is necessary to obtain the observed DM relic density since the ‘direct’ reactions $\bar{\chi}_{1(2)}\chi_{1(2)} \rightarrow V^* \rightarrow e^+e^-$ do not occur at lowest order in g_D .

As is well-known [45], the co-annihilation process cross section for $\bar{\chi}_1\chi_2 + h.c. \rightarrow V^* \rightarrow e^+e^-$ at freeze-out is suppressed by a factor of $\lambda = 2F/(1+F)^2$ [45], where $F = (1+\delta)^{3/2}e^{-\delta x_f}$, in comparison to the naive calculation due to the thermally suppressed χ_2 distribution. For $\delta = 0.1(0.2, 0.3)$ one finds that $F = 0.156(0.024, 0.0037)$, assuming that $x_f = 20$, and which falls quite rapidly as δ increases further and hence the reason why small values of δ are preferred in obtaining sufficiently large cross sections. In the non-relativistic limit for this s -wave process we find that this annihilation cross section, using the notation above (but now with $r = m_1/m_V$), is given by

$$\sigma_{DM}v_{rel} = 34.1 \lambda \sigma_0 \left(\frac{g_D \epsilon}{10^{-4}} \right)^2 \left(\frac{100 \text{ MeV}}{m_V} \right)^2 \frac{r^2(1+\delta)}{[r^2(2+\delta)^2 - 1]^2 + G^2}. \quad (9)$$

Here we have assumed that the contributions to $\langle \sigma_{DM}v_{rel} \rangle$ from both the $\bar{\chi}_1\chi_1$ and $\bar{\chi}_2\chi_2$ channels can be neglected since they appear only at higher order in g_D^2 . Taking, *e.g.*, $\delta = 0.1(0.2)$ with $m_V = 100$ MeV, $r = 0.75$ and $g_D \epsilon = 3 \times 10^{-4}$, similar to that employed above, and performing the thermal average explicitly we find that $\langle \sigma_{DM}v_{rel} \rangle \simeq 11.6(1.84)\sigma_0$ where the ‘target’ value to explain the observed DM relic density is $\simeq 4.4\sigma_0$ [13, 14] thus demonstrating that the required cross section is readily achievable⁶. The cross sections for the more general case can be obtained by using the results found in Fig. 3 as a function of $r > 1/2$ for different values of δ and then simply rescaling using the equation above but with the possible addition of the terms appearing in the square bracket in Eq.(3) depending upon the DP mass. It is clear from this Figure that for δ much greater than ~ 0.2 or so it is difficult to obtain the observed relic density for DM and DP in this mass range.

At later times, *e.g.*, during the CMB (at roughly $z \sim 10^3$), this cross section is suppressed by a factor of order $\sim e^{-\delta x_f(T_{FO}/T_{CMB})}$ as previously noted so that the CMB constraints are simultaneously very easily satisfied. We note that if $m_1 > m_V$ then the s -channel cross section for $\bar{\chi}_1\chi_1 \rightarrow 2V$ with V on-shell is no longer ϵ^2 suppressed and can easily lead to conflict with CMB constraints as was the case for $\phi^\dagger\phi \rightarrow 2V$ above; thus we have maintained the requirement that $r < 1$ in our calculations here to avoid this issue.

⁵Note that in our notation χ_1 is the lighter state and we will for simplicity assume that $m_M < m_D$ here.

⁶For smaller values of δ , *e.g.*, 0.01, cross sections larger by a factor of $\simeq 2.7$ may be achieved for this value or r .

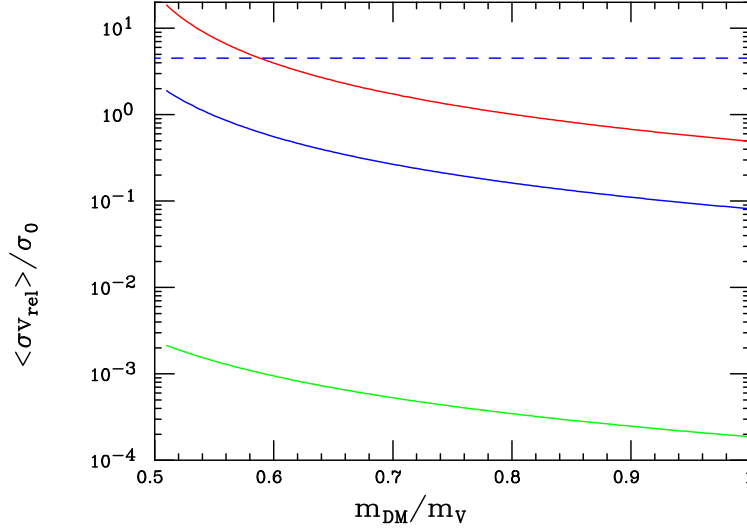


Figure 3: The thermally averaged value of $\sigma_{DM}v_{rel}$ for the case of pseudo-Dirac DM for the same parameter choices as made as in Fig. 1 assuming $r = m_{DM}/m_V > 1/2$ and with annihilation solely to the e^+e^- final state. The top(middle, lower) curve corresponds to the choices $\delta = 0.1(0.2, 0.3)$, respectively.

With DP ISR, the s -wave process $\bar{\chi}_1\chi_1 \rightarrow VV^*, V^* \rightarrow e^+e^-$ becomes possible when $1/2 < r < 1$ where the χ_2 is now exchanged in the t - and u -channels; the corresponding process with χ_1 interchanged with χ_2 still remains doubly Boltzmann suppressed. One may worry that the Majorana mass term above now allows for a potentially large coupling $\sim m_m/v_s$ of $\bar{\chi}_1\chi_1$ to S so that S -exchange itself could directly mediate the $\bar{\chi}_1\chi_1 \rightarrow VV^*$ process. While true, it is easy to convince oneself that this process is necessarily dominantly p -wave and so is suppressed by v_{rel}^2 at the later CMB times of relevance here.

Again employing the non-relativistic limit, we can obtain the $\bar{\chi}_1\chi_1 \rightarrow VV^*, V^* \rightarrow e^+e^-$ annihilation rate now given by

$$\sigma_{DM}v_{rel} = 3.96 \times 10^{-2} \sigma_0 \left(\frac{g_D}{e}\right)^2 \left(\frac{g_D\epsilon}{10^{-4}}\right)^2 \left(\frac{100\text{MeV}}{m_V}\right)^2 v^2 J, \quad (10)$$

where $v = m_V/2m_1$ and J is the phase space integral

$$J = \int_0^{(1-v)^2} dx_{12} \int_{min}^{max} dx_{23} \frac{(1-x_{12}+v^2)[(1-x_{13})(x_{13}-v^2)+(1 \rightarrow 2)] - (x_{13}-v^2)(x_{23}-v^2)(1+v^2)}{[(x_{12}-v^2)^2 + (Gv^2)^2][1-x_{12}-v^2+(z^2-1)2]^2}, \quad (11)$$

where we follow the same notation as above and also define the quantities $z = m_2/m_1 = 1 + \delta$ and $x_{13} = 1 + v^2 - x_{12} - x_{23} = 1 - E_e/m_1$. The top panel of Fig. 4 shows the numerical results for this cross section as a function of v for various values of $\delta = z - 1$. Taking, *e.g.*, $r = 0.75$, $g_D = g_{wk}$ and $g_D\epsilon = 3 \times 10^{-4}$, as above, for purposes of demonstration, we find that $\sigma_{DM}v_{rel} \simeq 4.83(3.41, 1.40, 0.44, 0.10, 0.011) \times 10^{-28} \text{ cm}^3\text{s}^{-1}$ for $\delta = 0.1, 0.2, 0.5, 1, 2$ and 4 , respectively⁷. Comparing with the rough cross section limit from the CMB above [25] for this DM mass we see that smaller values of δ now become excluded for these parameter choices. This implies that possible tension with the CMB constraints for smaller values of δ is more likely in this scenario than that found earlier in the previously considered case of complex scalar DM.

In the lower panel of Fig. 4, we see the present and potential future bounds on the parameter η introduced above for the range $\delta = 0.1 - 2$. Also shown are the predictions for the above benchmark

⁷For smaller values of δ , *e.g.*, 0.01 corresponding to $z = 1.01$, cross sections larger by a factor of $\simeq 1.3$ can be achieved with this assumed value of r .

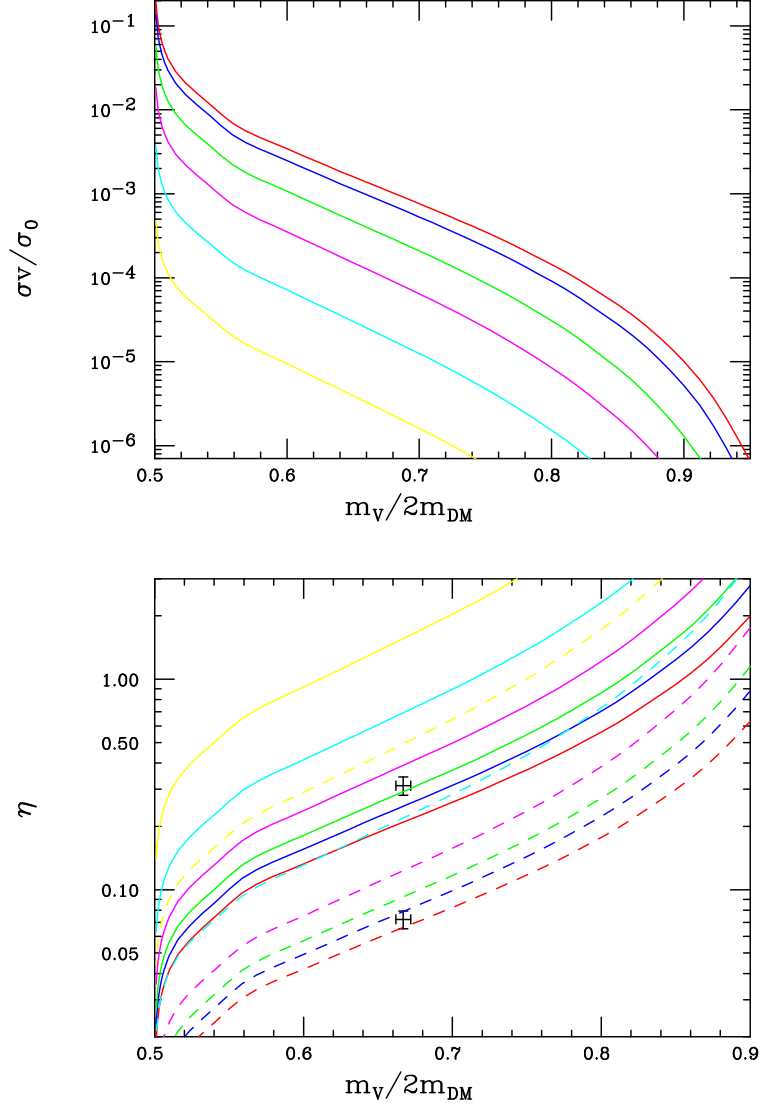


Figure 4: (Top) $\sigma_{DM}v_{rel}$ as a function of $v = m_V/2m_1$ for various values of δ . From top to bottom, the curves correspond to the values of $\delta = 0.1, 0.2, 0.5, 1, 2$ and 4 , respectively. As above, the values of $m_V = 100$ MeV, $g_D/e = 1$ and $g_D\epsilon = 10^{-4}$ have been assumed. (Bottom) Present (solid) and potential future (dash) bound on the parameter η as defined in the text as a function of v for, from bottom to top, $\delta = 0.1, 0.2, 0.3, 0.5, 1$ and 2 , respectively. As above, the benchmarks shown correspond to the two parameter choices discussed in the text where $g_D = g_{wk}(e)$ is the upper (lower) point as is described above.

points with $r = 0.75$, $m_V = 100$ MeV and $g_D \epsilon = 3 \times 10^{-4}$ when we take either $g_D = g_{wk}$ or $g_D = e$ corresponding to the upper or lower data point. Here we see that for $\delta \lesssim 0.3$, the former choice of $g_D = g_{wk}$ is already excluded by the existing data while improvements in the bounds from the CMB measurements may eventually exclude larger values up to roughly $\delta \lesssim 2$ and possibly also exclude the latter choice of coupling strength, $g_D = e$, when $\delta \lesssim 0.15$. Clearly the CMB constraints will place reasonable constraints on the parameter space of this model.

4 Discussion and Summary

The kinetic mixing model with both dark photons and dark matter in the sub-GeV mass range poses an interesting alternative to the well-studied traditional WIMP and axion scenarios. However, constraints from the CMB can pose significant model building requirements on this class of models in that the annihilation process by which the DM achieves the observed relic density cannot be dominantly s -wave, or more generally, temperature-independent. Annihilation via a p -wave process, as in the case of complex scalar DM, or via co-annihilation, as in the case of pseudo-Dirac DM with a small mass splitting, offer two attractive alternative setups that circumvent these constraints. In both these scenarios, the emission of additional dark ISR in the form of a DP as part of the annihilation process, though higher order in α_D , necessarily leads to a numerically suppressed s -wave process with a rate that is insufficient to explain the DM relic density but may still be in conflict with the bounds from the CMB in certain parameter space regimes. This leads to an additional set of constraints on the model space of these scenarios and, in this paper, we performed a preliminary examination of the impact of these constraints arising from the rate for the emission of this additional DP. Indeed, potentially important constraints were obtained for both the charged scalar and pseudo-Dirac scenarios, particularly in the later case when the mass splitting between the two eigenstates is small as it must be to generate the observed relic density. These dark ISR constraints were found to scale with the general model parameters roughly as $\sim \epsilon \alpha_D m_V^{-3/2} \mathcal{G}$, where \mathcal{G} is a dimensionless function of the ratio of the DM and DP masses, m_{DM}/m_V and possibly other specific model dependent parameters, such as the mass splitting between the two pseudo-Dirac states encountered above. Future improvements in the measurements of the CMB by the next generation of experiments were also shown to be able to significantly strengthen these present bounds in specific directions in the model parameter space.

Further detailed study of the effects of the CMB constraints and dark ISR on the parameter spaces of DM models is clearly warranted.

5 Acknowledgements

The author would like to thank J.L. Hewett, D. Rueter and G. Wojcik for valuable discussions related to this analysis. This work was supported by the Department of Energy, Contract DE-AC02-76SF00515.

References

- [1] G. Arcadi, M. Dutra, P. Ghosh, M. Lindner, Y. Mambrini, M. Pierre, S. Profumo and F. S. Queiroz, *Eur. Phys. J. C* **78**, no.3, 203 (2018) [arXiv:1703.07364 [hep-ph]].
- [2] L. Roszkowski, E. M. Sessolo and S. Trojanowski, *Rept. Prog. Phys.* **81**, no.6, 066201 (2018) [arXiv:1707.06277 [hep-ph]].
- [3] M. Kawasaki and K. Nakayama, *Ann. Rev. Nucl. Part. Sci.* **63**, 69 (2013) [arXiv:1301.1123 [hep-ph]].

- [4] P. W. Graham, I. G. Irastorza, S. K. Lamoreaux, A. Lindner and K. A. van Bibber, *Ann. Rev. Nucl. Part. Sci.* **65**, 485 (2015) [arXiv:1602.00039 [hep-ex]].
- [5] I. G. Irastorza and J. Redondo, *Prog. Part. Nucl. Phys.* **102**, 89-159 (2018) [arXiv:1801.08127 [hep-ph]].
- [6] K. Pachal, “Dark Matter Searches at ATLAS and CMS”, given at the 8th *Edition of the Large Hadron Collider Physics Conference*, 25-30 May, 2020.
- [7] E. Aprile *et al.* [XENON], *Phys. Rev. Lett.* **121**, no.11, 111302 (2018) doi:10.1103/PhysRevLett.121.111302 [arXiv:1805.12562 [astro-ph.CO]].
- [8] A. Albert *et al.* [Fermi-LAT and DES], *Astrophys. J.* **834**, no.2, 110 (2017) doi:10.3847/1538-4357/834/2/110 [arXiv:1611.03184 [astro-ph.HE]].
- [9] C. Amole *et al.* [PICO], *Phys. Rev. D* **100**, no.2, 022001 (2019) doi:10.1103/PhysRevD.100.022001 [arXiv:1902.04031 [astro-ph.CO]].
- [10] J. Alexander *et al.*, arXiv:1608.08632 [hep-ph].
- [11] M. Battaglieri *et al.*, arXiv:1707.04591 [hep-ph].
- [12] G. Bertone and T. Tait, M.P., *Nature* **562**, no.7725, 51-56 (2018) [arXiv:1810.01668 [astro-ph.CO]].
- [13] G. Steigman, *Phys. Rev. D* **91**, no. 8, 083538 (2015) [arXiv:1502.01884 [astro-ph.CO]].
- [14] K. Saikawa and S. Shirai, [arXiv:2005.03544 [hep-ph]].
- [15] B. Holdom, *Phys. Lett.* **166B**, 196 (1986) and *Phys. Lett. B* **178**, 65 (1986); K. R. Dienes, C. F. Kolda and J. March-Russell, *Nucl. Phys. B* **492**, 104 (1997) [hep-ph/9610479]; F. Del Aguila, *Acta Phys. Polon. B* **25**, 1317 (1994) [hep-ph/9404323]; K. S. Babu, C. F. Kolda and J. March-Russell, *Phys. Rev. D* **54**, 4635 (1996) [hep-ph/9603212]; T. G. Rizzo, *Phys. Rev. D* **59**, 015020 (1998) [hep-ph/9806397].
- [16] There has been a huge amount of work on this subject; see, for example, D. Feldman, B. Kors and P. Nath, *Phys. Rev. D* **75**, 023503 (2007) [hep-ph/0610133]; D. Feldman, Z. Liu and P. Nath, *Phys. Rev. D* **75**, 115001 (2007) [hep-ph/0702123 [HEP-PH]].; M. Pospelov, A. Ritz and M. B. Voloshin, *Phys. Lett. B* **662**, 53 (2008) [arXiv:0711.4866 [hep-ph]]; M. Pospelov, *Phys. Rev. D* **80**, 095002 (2009) [arXiv:0811.1030 [hep-ph]]; H. Davoudiasl, H. S. Lee and W. J. Marciano, *Phys. Rev. Lett.* **109**, 031802 (2012) [arXiv:1205.2709 [hep-ph]] and *Phys. Rev. D* **85**, 115019 (2012) doi:10.1103/PhysRevD.85.115019 [arXiv:1203.2947 [hep-ph]]; R. Essig *et al.*, arXiv:1311.0029 [hep-ph]; E. Izaguirre, G. Krnjaic, P. Schuster and N. Toro, *Phys. Rev. Lett.* **115**, no. 25, 251301 (2015) [arXiv:1505.00011 [hep-ph]]; M. Khlopov, *Int. J. Mod. Phys. A* **28**, 1330042 (2013) [arXiv:1311.2468 [astro-ph.CO]]; For a general overview and introduction to this framework, see D. Curtin, R. Essig, S. Gori and J. Shelton, *JHEP* **1502**, 157 (2015) [arXiv:1412.0018 [hep-ph]].
- [17] M. Fabbri, E. Gabrielli and G. Lanfranchi, [arXiv:2005.01515 [hep-ph]].
- [18] T. G. Rizzo, *Phys. Rev. D* **99**, no.11, 115024 (2019) [arXiv:1810.07531 [hep-ph]].
- [19] T. D. Rueter and T. G. Rizzo, *Phys. Rev. D* **101**, no.1, 015014 (2020) [arXiv:1909.09160 [hep-ph]].
- [20] J. H. Kim, S. D. Lane, H. S. Lee, I. M. Lewis and M. Sullivan, *Phys. Rev. D* **101**, no.3, 035041 (2020) [arXiv:1904.05893 [hep-ph]].
- [21] N. Sabti, J. Alvey, M. Escudero, M. Fairbairn and D. Blas, *JCAP* **01**, 004 (2020) [arXiv:1910.01649 [hep-ph]].
- [22] N. Aghanim *et al.* [Planck Collaboration], arXiv:1807.06209 [astro-ph.CO].
- [23] H. Liu, T. R. Slatyer and J. Zavala, *Phys. Rev. D* **94**, no. 6, 063507 (2016) [arXiv:1604.02457 [astro-ph.CO]].

- [24] R. K. Leane, T. R. Slatyer, J. F. Beacom and K. C. Ng, Phys. Rev. D **98**, no.2, 023016 (2018) doi:10.1103/PhysRevD.98.023016 [arXiv:1805.10305 [hep-ph]].
- [25] J. Cang, Y. Gao and Y. Z. Ma, [arXiv:2002.03380 [astro-ph.CO]].
- [26] N. F. Bell, J. B. Dent, T. D. Jacques and T. J. Weiler, Phys. Rev. D **78**, 083540 (2008) [arXiv:0805.3423 [hep-ph]].
- [27] M. Kachelriess, P. Serpico and M. Solberg, Phys. Rev. D **80**, 123533 (2009) [arXiv:0911.0001 [hep-ph]].
- [28] T. Bringmann, X. Huang, A. Ibarra, S. Vogl and C. Weniger, JCAP **07**, 054 (2012) [arXiv:1203.1312 [hep-ph]].
- [29] N. F. Bell, Y. Cai, J. B. Dent, R. K. Leane and T. J. Weiler, Phys. Rev. D **96**, no.2, 023011 (2017) [arXiv:1705.01105 [hep-ph]].
- [30] P. Adrian *et al.* [HPS], Phys. Rev. D **98**, no.9, 091101 (2018) [arXiv:1807.11530 [hep-ex]].
- [31] A. Casais Vidal [LHCb], PoS **LHCP2019**, 180 (2019)
- [32] A. Ariga *et al.* [FASER], [arXiv:1901.04468 [hep-ex]].
- [33] D. Banerjee *et al.* [NA64], Phys. Rev. D **101**, no.7, 071101 (2020) [arXiv:1912.11389 [hep-ex]].
- [34] H. Lubatti *et al.* [MATHUSLA], [arXiv:1901.04040 [hep-ex]].
- [35] M. Campajola [Belle II], PoS **LeptonPhoton2019**, 063 (2019)
- [36] C. Ahdida *et al.* [SHiP], [arXiv:2002.08722 [physics.ins-det]].
- [37] T. Akesson *et al.* [LDMX], [arXiv:1808.05219 [hep-ex]]. See also, A. Berlin, N. Blinov, G. Krnjaic, P. Schuster and N. Toro, Phys. Rev. D **99**, no.7, 075001 (2019) [arXiv:1807.01730 [hep-ph]].
- [38] ATLAS Collaboration, “Search for invisible Higgs boson decays with vector boson fusion signatures with the ATLAS detector using an integrated luminosity of 139 fb^{-1} ,” ATLAS-CONF-2020-008.
- [39] A. Berlin, D. Hooper and S. D. McDermott, Phys. Rev. D **89**, no.11, 115022 (2014) [arXiv:1404.0022 [hep-ph]].
- [40] J. L. Feng and J. Smolinsky, Phys. Rev. D **96**, no. 9, 095022 (2017) [arXiv:1707.03835 [hep-ph]] .
- [41] B. Li and Y. F. Zhou, Commun. Theor. Phys. **64**, no. 1, 119 (2015) [arXiv:1503.08281 [hep-ph]]
- [42] D. Tucker-Smith and N. Weiner, Phys. Rev. D **64**, 043502 (2001) [arXiv:hep-ph/0101138 [hep-ph]].
- [43] A. De Simone, V. Sanz and H. P. Sato, Phys. Rev. Lett. **105**, 121802 (2010) [arXiv:1004.1567 [hep-ph]].
- [44] R. Krall and M. Reece, Chin. Phys. C **42**, no.4, 043105 (2018) [arXiv:1705.04843 [hep-ph]].
- [45] K. Griest and D. Seckel, Phys. Rev. D **43**, 3191-3203 (1991) doi:10.1103/PhysRevD.43.3191